Dynamics of the Milky Way: an observational and modelling perspective

Eugene Vasiliev

Institute of Astronomy, Cambridge

Linking the Galactic and Extragalactic workshop, 28 November 2022

artwork by Clifford Possum Tjapaltjarri

Outline

Observational facilities:

Measurements:

distance, velocity, chemistry, stellar parameters; density and kinematic distributions . . .

Modelling approaches:

Jeans equations, distribution functions, orbit- and particle-based models, stellar streams, non-equilibrium effects

Objectives:

gravitational field of the Milky Way;
origin and properties of different dynamical components

Distance measurement

Gaia provides 5d astrometric data for $\sim 1.5 \times 10^9$ stars, but. . .

measured parallax $\varpi \sim \mathcal{N}(1/D + \varpi_0,\ \epsilon_\varpi)$, with the zero-point $\varpi_0 \simeq -0.01$ mas varying across the sky and CMD, and measurement uncertainty becoming too large beyond a few kpc.

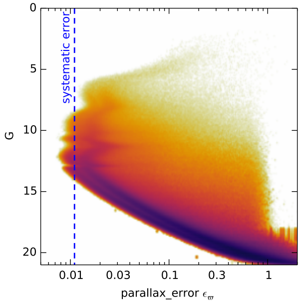

Cutting the catalogue on the "signal-to-noise ratio" ϖ/ϵ_ϖ introduces biases [Luri+ 2018] and dramatically reduces the number of stars.

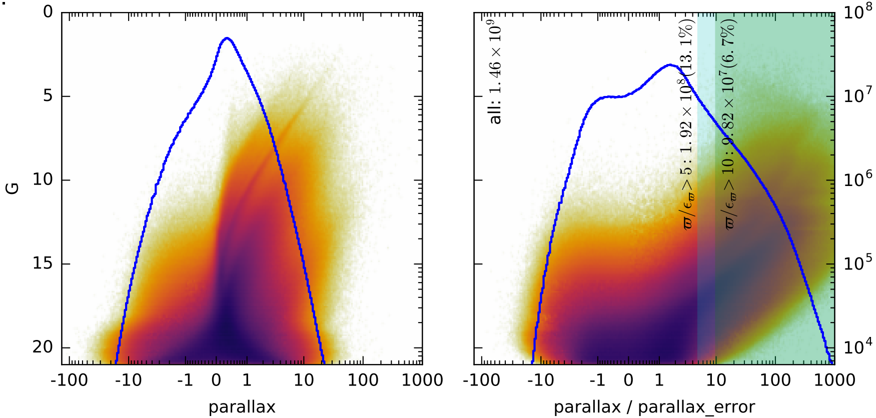

Distance measurement

Of course, in many applications one may need only the brighter stars, whose parallaxes are more precise, but even for $G < 18.5$ most stars have $\varpi/\epsilon_\varpi < 5$.

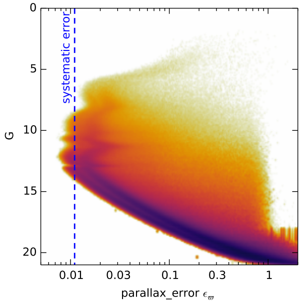

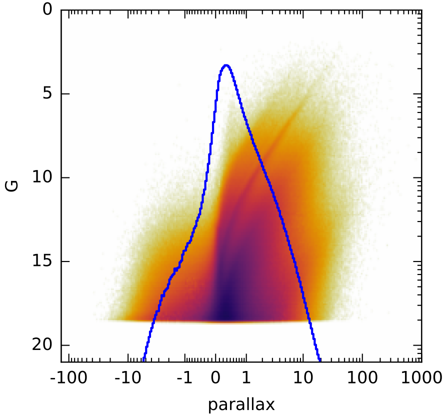

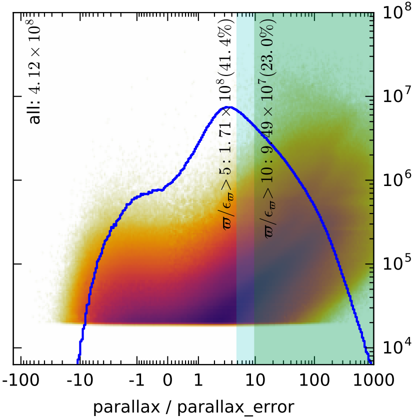

Distance measurement

However, when combining parallax with photometry, one can hope to achieve much better precision especially for faint stars.

StarHorse [Anders+ 2022] is one of several alternative catalogues, but is still based on EDR3 astrometry.

Gaia DR3 itself contains a `distance` column, but it comes with a number of caveats and can only be trusted up to a few kpc. Several groups declared intent to provide alternative and better calibrated distance catalogues, using BP–RP spectra.

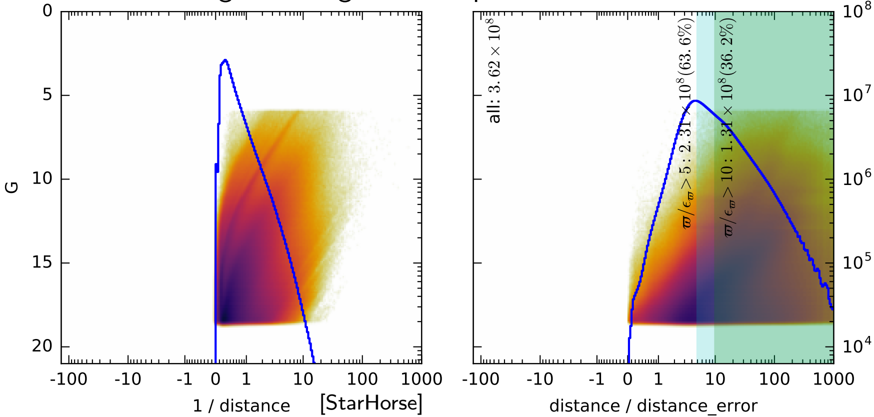

Distance measurement

On the other hand, if one considers the Gaia RVS catalogue ($G \lesssim 16$), parallaxes are mostly precise enough, and additional cut on S/N does not significantly reduce the sample size.
Of course, it is still limited to a few kpc...

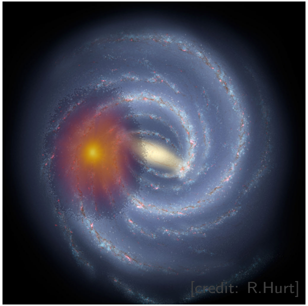

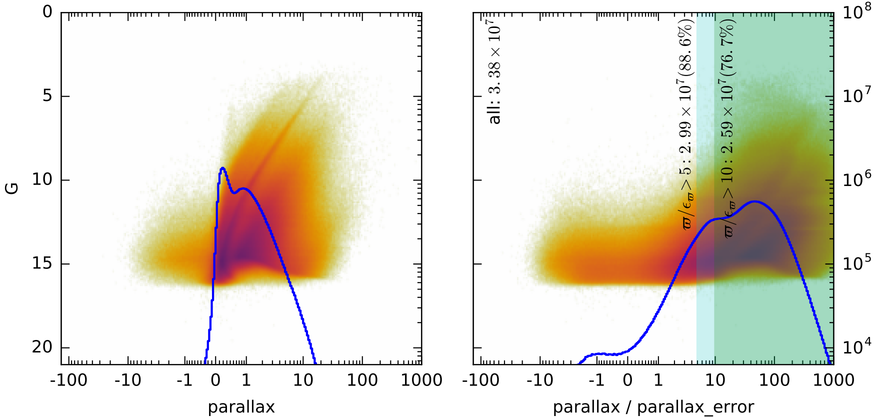

Spectroscopic surveys

Gaia RVS is the largest dataset ($\gtrsim 3 \times 10^7$ stars), all-sky but limited to bright stars;
other surveys (in particular APOGEE and Gaia–ESO) go deeper and provide detailed chemistry in addition to V_{LOS}.

number of stars in common [thousands]

	Gaia	LAMOST_LR	LAMOST_MR	APOGEE	GALAH	RAVE	SDSS
Gaia	29266	2378	401	436	437	398	5.6
LAMOST_LR	2378	4637	240	122	36	8.3	39
LAMOST_MR	401	240	433	32	13	0.98	0.27
APOGEE	436	122	32	556	30	16	0.88
GALAH	437	36	13	30	450	22	0.099
RAVE	398	8.3	0.98	16	22	410	0.005
SDSS	5.6	39	0.27	0.88	0.099	0.005	505

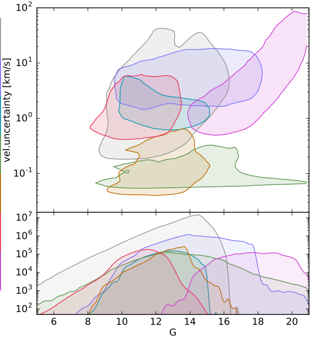

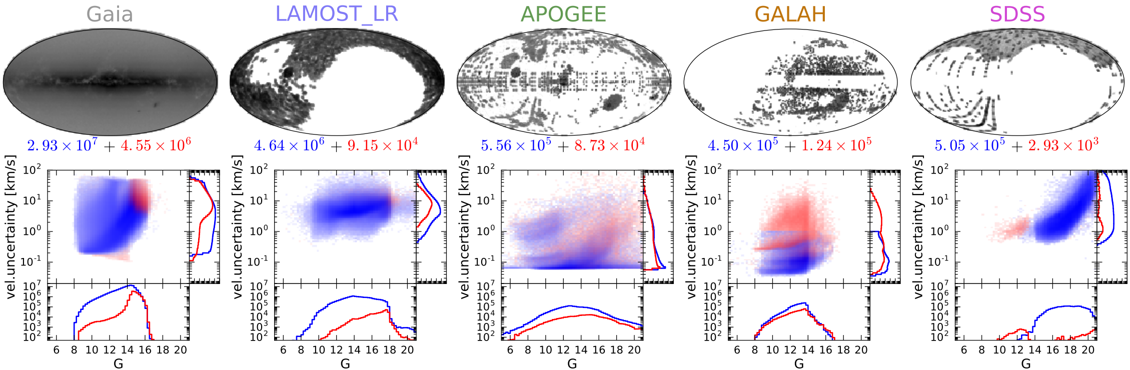

Sky-plane velocity measurement

$$\frac{V}{1\,\mathrm{km/s}} = 4.74\,\frac{\mu}{1\,\mathrm{mas/yr}}\,\frac{D}{1\,\mathrm{kpc}}$$

(if the distance is known perfectly)

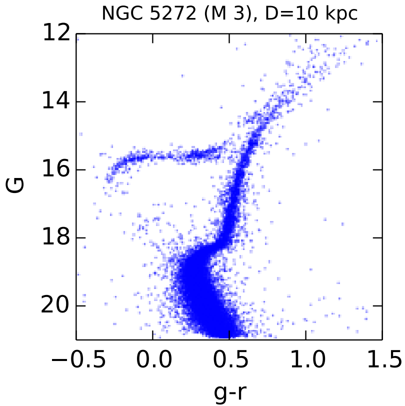

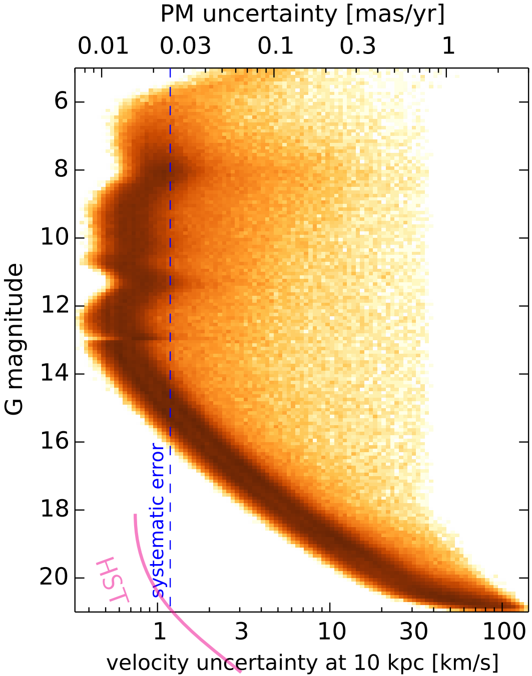

Sky-plane velocity measurement

$$\frac{V}{1\,\mathrm{km/s}} = 4.74\,\frac{\mu}{1\,\mathrm{mas/yr}}\,\frac{D}{1\,\mathrm{kpc}}$$

In general, the velocity uncertainty has contribution from both PM and distance uncertainties:

$$\epsilon_V = \epsilon_\mu\, D + \frac{\epsilon_D}{D}\, V$$

If distance is measured from parallax:

$$\epsilon_V = \epsilon_\mu\, D + \frac{\epsilon_\varpi}{\varpi}\, V = (\epsilon_\mu + \epsilon_\varpi\, V)\, D$$

dominates if $V \gtrsim 5$ km/s

$$\epsilon_\varpi \simeq \epsilon_\mu \gtrsim 0.01 \text{ mas or mas/yr}$$

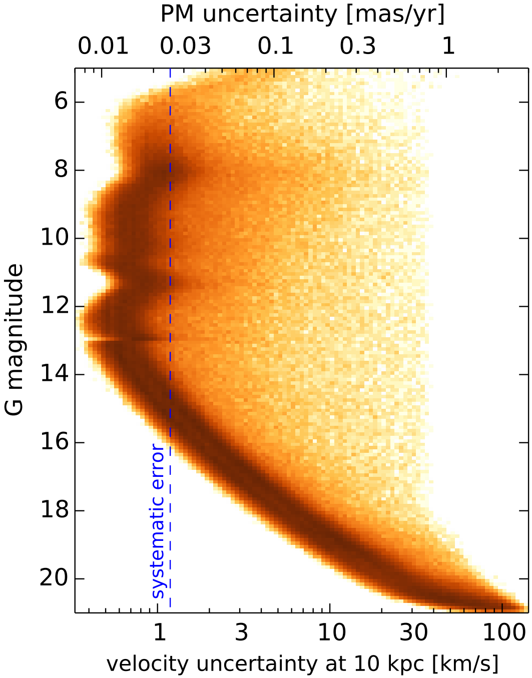

.5

Sky-plane velocity measurement

$$\frac{V}{1\,\mathrm{km/s}} = 4.74\,\frac{\mu}{1\,\mathrm{mas/yr}}\,\frac{D}{1\,\mathrm{kpc}}$$

In general, the velocity uncertainty has contribution from both PM and distance uncertainties:

$$\epsilon_V = \epsilon_\mu\, D + \frac{\epsilon_D}{D}\, V$$

If distance is inferred from photometry with a relative uncertainty $\eta \equiv \epsilon_D/D \approx \mathrm{const}$ (e.g., for RR Lyrae $\eta \simeq 0.1$):

$$\epsilon_V = \epsilon_\mu\, D + \eta\, V$$

dominates if $D \gtrsim 25$ kpc

fixed (~ 10 km/s)

However, since $\epsilon_\mu \propto T^{-3/2}$, it will be 2.5× lower in DR4

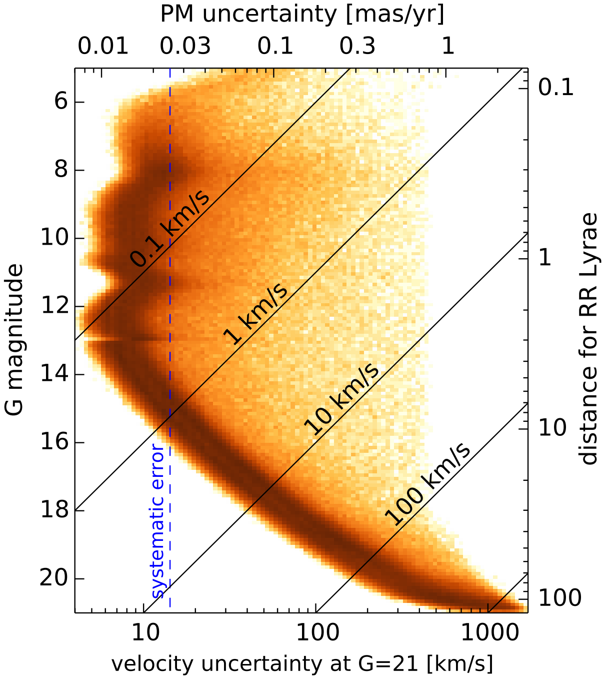

Density profile measurement

. . . is much more difficult than just "counting the stars": one needs to account for their luminosity function, spatial and magnitude coverage of the survey and various other biases.

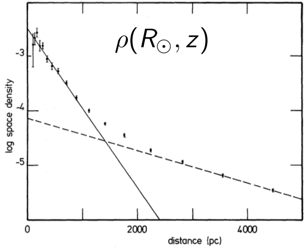

[Gilmore & Reid 1983]

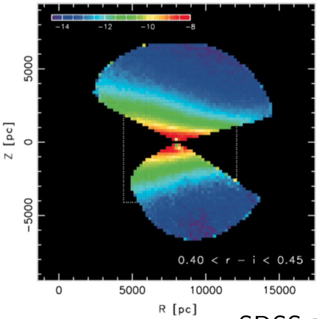

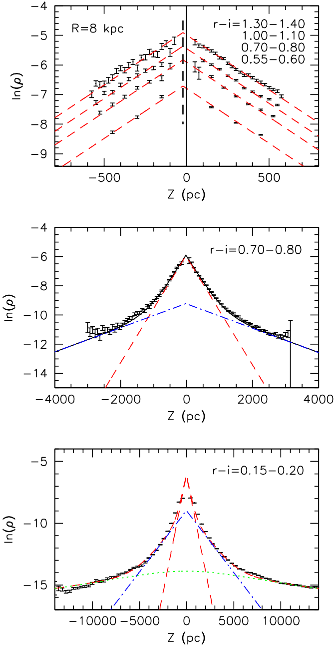

SDSS [Jurić+ 2008]

Density profile measurement

The entire Milky Way contains $\sim 10^{11}$ stars, but the vast majority of them are too faint to be observed (at least by Gaia).

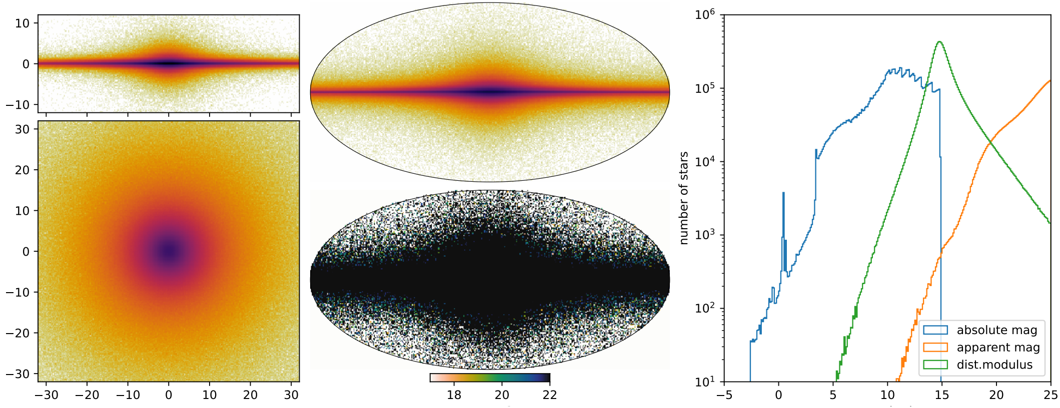

Density profile measurement

The selection function of a survey is the probability that a star with given properties (e.g., position α, δ and apparent magnitude G) enters the catalogue (see Everall & Das 2020, Rix+ 2022 for a general discussion). For Gaia DR2, the selection function was derived in a series of papers by Boubert & Everall, and the GaiaUnlimited collaboration is developing a toolbox for the latest and future data releases.

The photometric catalogue is nearly complete at $G < G_{50\%}(\alpha, \beta) \lesssim 21$.

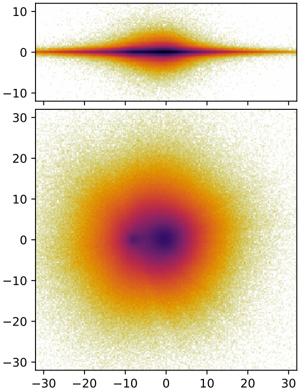

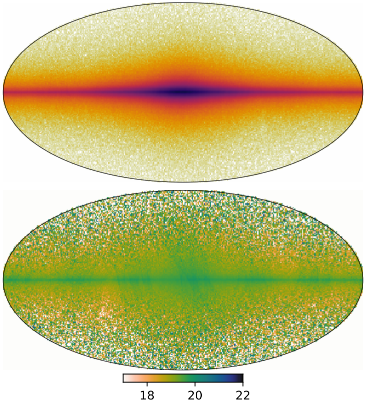

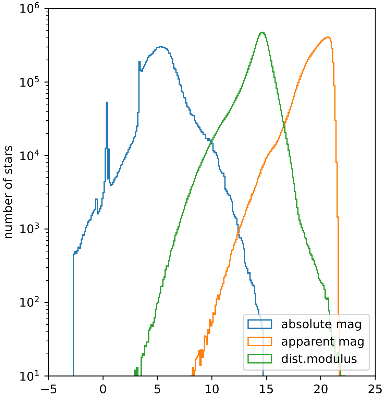

Density profile measurement

If we assume the selection function to be known, then the parameters of the density distribution can be optimized to maximize the likelihood of observing the given catalogue.

In reality, the dust extinction limits the observable volume even further, but the general problem of simultaneously inferring *both* the 3d density profile *and* the 3d extinction map is extremely challenging!

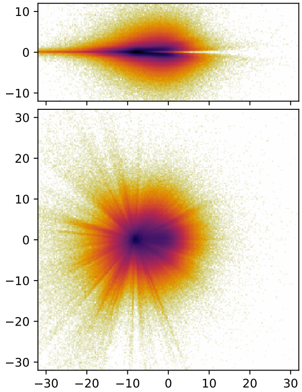

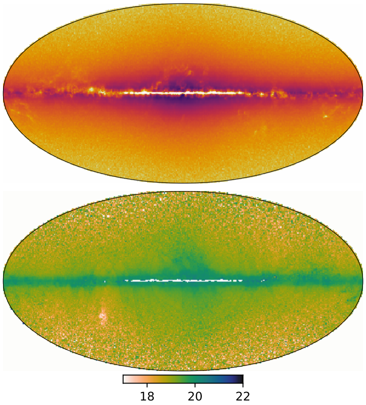

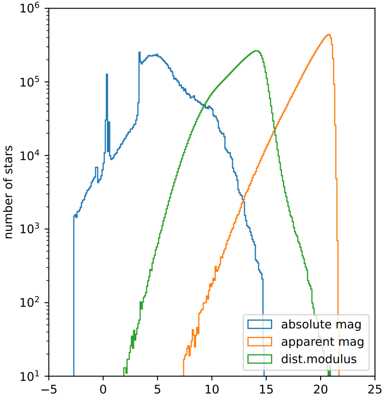

Density profile measurement

For instance, in a recent study Everall+ 2022a,b considered just the two narrow cone around Galactic poles, which is nearly dust-free, and made a number of further simplifications regarding the distribution of stars in absolute magnitudes. Then the observed distribution of parallaxes and apparent magnitudes was used to measure the vertical density profile $\rho(R_\odot, z)$.

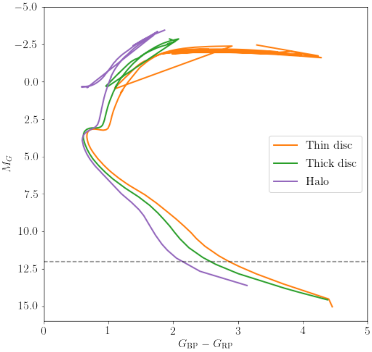

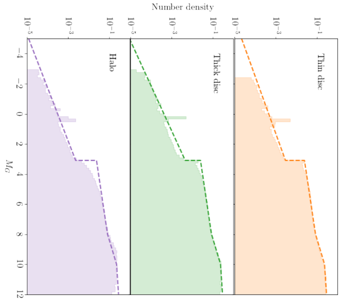

Ideally one needs to perform this fit in a larger volume, using colours and proper motion information to distinguish nearby dwarfs from distant giants.

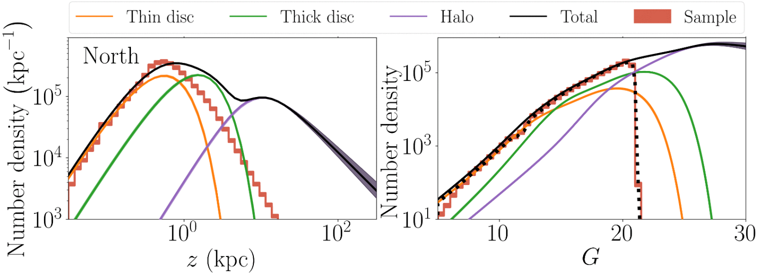

Basics of dynamical modelling

Goal: determine the mass distribution of a stellar system from the kinematics of some tracer population(s), whose distribution function $f(\mathbf{x}, \mathbf{v}, t)$ satisfies the collisionless Boltzmann equation:

$$\frac{\partial f(\mathbf{x}, \mathbf{v}, t)}{\partial t} + \mathbf{v}\,\frac{\partial f(\mathbf{x}, \mathbf{v}, t)}{\partial \mathbf{x}} - \frac{\partial \Phi(\mathbf{x}, t)}{\partial \mathbf{x}}\,\frac{\partial f(\mathbf{x}, \mathbf{v}, t)}{\partial \mathbf{v}} = 0.$$

Potential $\Leftrightarrow$ mass distribution

not measured directly on human timescales

In order to infer anything about the potential from a time-dependent DF, need to make further assumptions about the initial state of the system, e.g., that the stars belong to a single stream or were perturbed from an equilibrium configuration in a specific way, etc.

Basics of dynamical modelling

Goal: determine the mass distribution of a stellar system from the kinematics of some tracer population(s), whose distribution function $f(\mathbf{x}, \mathbf{v}, t)$ satisfies the collisionless Boltzmann equation:

$$\mathbf{v}\,\frac{\partial f(\mathbf{x}, \mathbf{v}\quad)}{\partial \mathbf{x}} - \frac{\partial \Phi(\mathbf{x}\quad)}{\partial \mathbf{x}}\,\frac{\partial f(\mathbf{x}, \mathbf{v}\quad)}{\partial \mathbf{v}} = 0.$$

3D
(want to infer)

Steady-state assumption $\Longrightarrow$ Jeans theorem:

$$f(\mathbf{x}, \mathbf{v}) = f\left(\mathcal{I}(\mathbf{x}, \mathbf{v};\ \Phi)\right)$$

3D – 6D
(observed)

integrals of motion ($\leq$ 3D?), e.g., $\mathcal{I} = \{E, L, \ldots\}$

With fully 6d phase-space measurements, the potential is overconstrained!

Jeans modelling

2d Jeans models use the $\overline{v_\phi}$ and $\sigma_{R,\phi,z}$ profiles in the meridional plane under certain assumptions about the orientation of the velocity ellipsoid.
Its main advantage is simplicity, and main drawback is that it ignores the information about the shape of the velocity distribution, especially the asymmetric $f(v_\phi)$.

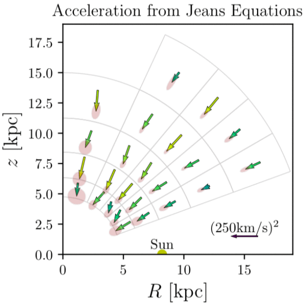

2d Jeans [Wegg+ 2019]

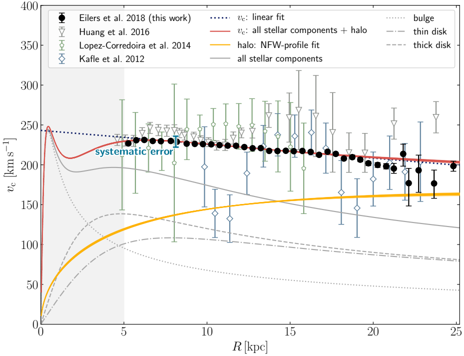

1d Jeans in R [Eilers+ 2019]

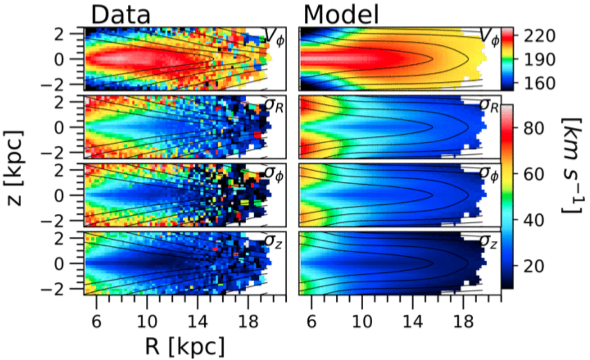

2d Jeans [Nitschai+ 2021]

Distribution function modelling

A general DF $f(\mathcal{I})$ is specified in terms of integrals of motion in the given potential $\mathcal{I}(\mathbf{x}, \mathbf{v};\ \Phi)$. To compute the density $\rho(\mathbf{x})$ generated by this DF, one needs to know $\Phi(\mathbf{x})$, but in the gravitationally self-consistent case, Φ is determined by ρ via the Poisson equation – thus we have a circular dependency.

Such models are constructed by the iterative approach [Prendergast & Tomer 1975; Rowley 1988; Kuijken & Dubinski 1995; Widrow+ 2005], which works best for action-based DFs [Binney 2014; Piffl+ 2015; Sanders & Evans 2016; Cole & Binney 2017; Vasiliev 2019]:

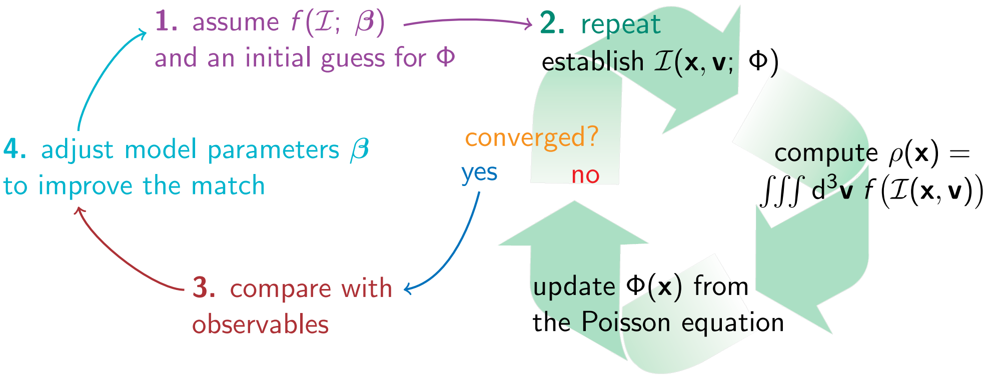

Distribution function modelling of the Galactic disc

DF-based models provide and are constrained by the entire velocity distribution function in multiple spatial bins, not just its first two moments. The number of stars in each spatial bin may be renormalized to match observations, circumventing the problem of dealing with spatial selection function. They also typically work with multiple DF components (split by age & chemistry).

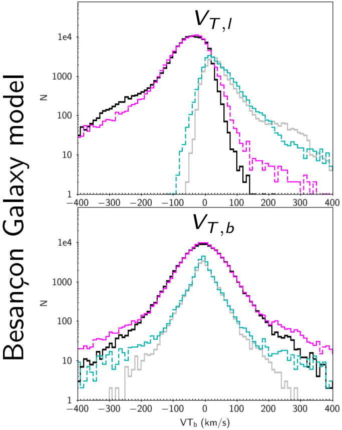

[Robin+ 2022]

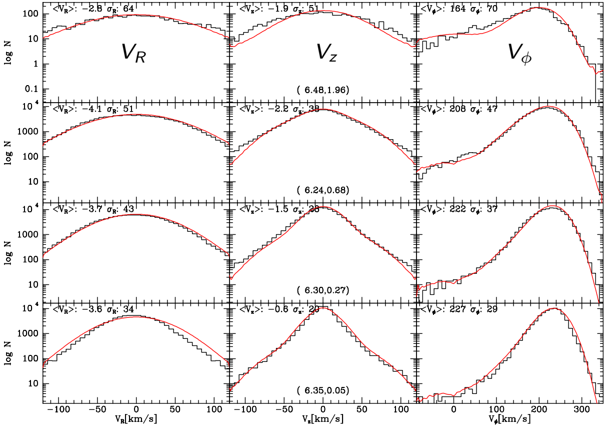

[Binney & Vasiliev 2022]

Dynamical modelling of halo stars, clusters and satellites

Discrete kinematic tracers at large distances ($\gtrsim$ 10 kpc) with 4–6d phase-space coords:

Stars in the outer halo (few$\times 10^3$ giants with V_{LOS}, $\sim 10^5$ RRL) [Xue+ 2008; Deason+ 2012, 2021; Hattori+ 2021; Shen+ 2022; Bird+ 2022].

Globular clusters ($\sim$ 150) [Eadie & Harris 2016; Watkins+ 2019; Vasiliev 2019; Posti & Helmi 2019; Eadie & Juric 2019; Wang+ 2022; Correa Magnus & Vasiliev 2022].

Satellite galaxies ($\lesssim$ 50) [Patel+ 2018; Callingham+ 2019; Li+ 2020; Cautun+ 2020; Fritz+ 2020; CM&V22; Slizewski+ 2022].

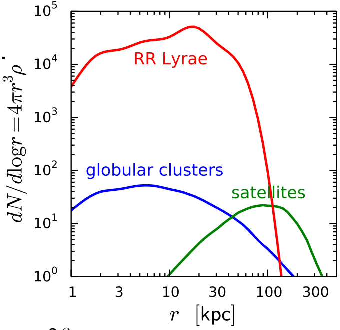

Methods:

Tracer mass estimator [Wilkinson & Evans 1999] – DF of the form $L^{-2\beta} f_E(E)$ constructed via Cuddeford–Eddington inversion for a power-law tracer density $\rho(r)$ in a power-law potential $\Phi(r)$.

Double-power-law DF in action space [Posti+ 2015; Williams+ 2015].

Empirical DF extracted from N-body simulations [e.g. Li+ 2017].

Common features: use unbinned datapoints, marginalize over measurement errors or missing phase-space dimensions.

Dynamical modelling of halo stars, clusters and satellites

stellar halo

total mass distribution

kinematics

density

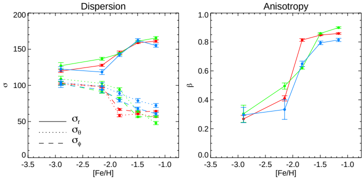

[Belokurov+ 2018]

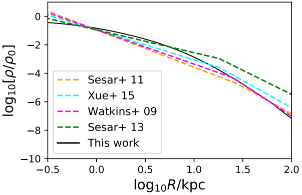

[Li&Binney 2021]

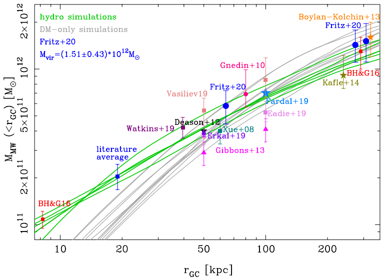

[Fritz+ 2020]

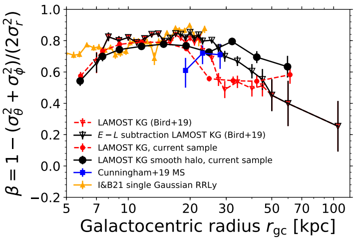

[Bird+ 2021]

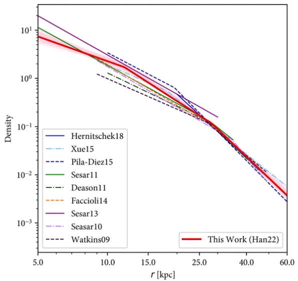

[Han+ 2022]

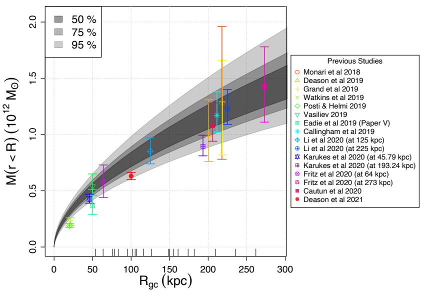

[Slizewski+ 2022]

M2M and Schwarzschild models

In both made-to-measure and Schwarzschild orbit-superposition methods, the DF in the space of integrals of motion $\mathcal{I}$ is represented as a weighted sum of delta-functions: $f(\mathcal{I}) = \sum_{i=1}^{N} m_i\, \delta(\mathcal{I} - \mathcal{I}_i)$, with $N \sim 10^3$–10^5 for orbit-based and $N \gtrsim 10^6$ for particle-based models.

Obviously these models are very flexible and are the only ones capable of representing rotating triaxial bars, thus have been applied for the Milky Way bulge/bar [Zhao 1996; Häfner+ 2000; Wang+ 2012], in particular to measure the bar pattern speed Ω_b [e.g. Portail+ 2015,2017].

One may replace numerically integrated orbits with tori in action space [McMillan & Binney 2013], though special care is needed for resonant regions.

Among advantages of orbit-based models, still awaiting to be realized, are the possibility to describe the rich substructures in the Galactic halo (ideally, building blocks from individual accretion episodes), and to deal with time-dependent potentials.

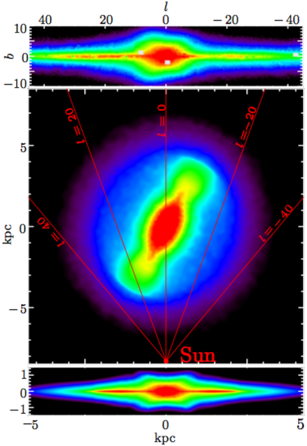

[Wegg+ 2016]

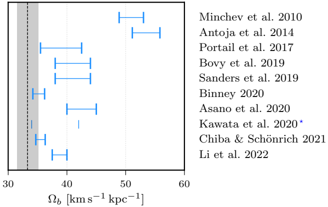

[Clarke & Gerhard 2022]

Constraining the Galactic potential directly from the CBE

1. Infer a smooth $f(\mathbf{x}, \mathbf{v})$ from the observed discrete samples (with uncertainties in $\mathbf{x}, \mathbf{v}$).
2. Measure the acceleration $\partial\Phi/\partial\mathbf{x}$ at different spatial locations $\mathbf{x}$ by fitting a linear least-squares regression to the DF derivatives (different values of $\mathbf{v}$ at a fixed $\mathbf{x}$ should give a consistent estimate of accelerations).

Still assume a stationary system, but ignore the Jeans theorem and sidestep the derivation of integrals of motion; seems to be more robust to deviations from equilibrium.

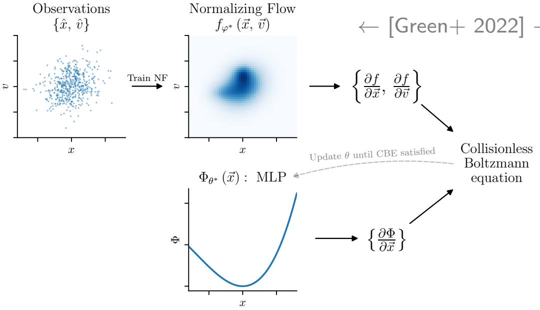

← [Green+ 2022] →

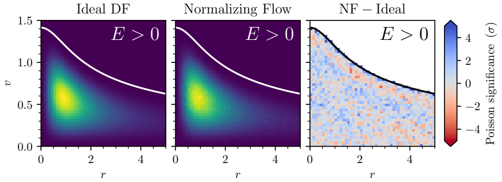

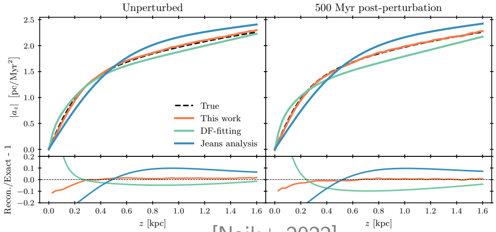

$$\text{CBE:} \quad \mathbf{v}\,\frac{\partial f(\mathbf{x},\mathbf{v})}{\partial \mathbf{x}} - \frac{\partial \Phi(\mathbf{x})}{\partial \mathbf{x}}\,\frac{\partial f(\mathbf{x},\mathbf{v})}{\partial \mathbf{v}} = 0$$

[Naik+ 2022]

Vertical perturbations in the Galactic disc

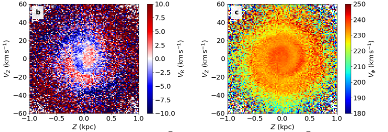

Gaia DR2 [Antoja+ 2018]

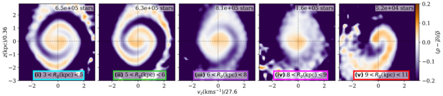

simulation [Gandhi+ 2022]

Leading theory: ripples after the impact of a massive satellite (implying Sgr dSph) through the disc [Widrow+ 2012; Laporte+ 2018,2019; Binney & Schönrich 2018; Li & Shen 2019; Bland-Hawthorn & Tepper-García 2021, etc.]

Caveat: Sgr was likely not massive enough at the time of the previous passage through the disc (1 Gyr ago) [Vasiliev & Belokurov 2020; Bennett+ 2022].

Counter-caveat: Sgr may have excited long-lived oscillations in the MW halo, which in turn perturb the disc [Grand+ 2022].

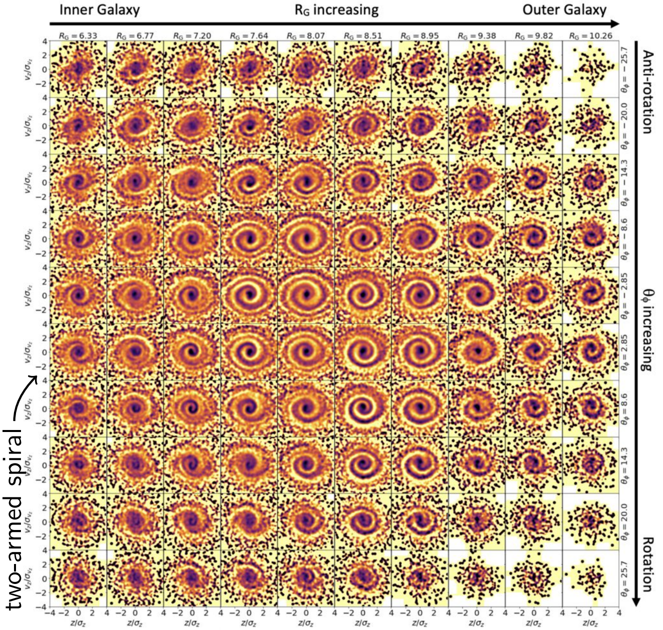

Gaia DR3 [Hunt+ 2022]

Constraining the Galactic potential by vertical perturbations

Obviously, these perturbations pose an obstacle for standard methods for measuring the potential (e.g., Jeans equations or DF fitting), but they can be used in a different way.

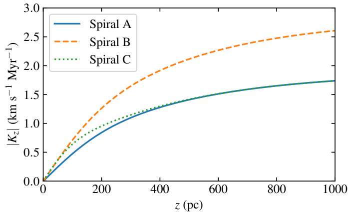

Assuming that the phase spiral is caused by an impulsive perturbation, its shape results from phase mixing in a non-harmonic potential (stars with low energy have higher frequency and are winding up faster). Thus the vertical potential ($\Leftrightarrow$ 1d mass distribution in the Galactic disc) can be inferred by fitting the shape of the spiral overdensity.

[Widmark+ 2019-2022]

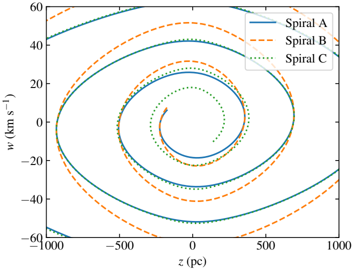

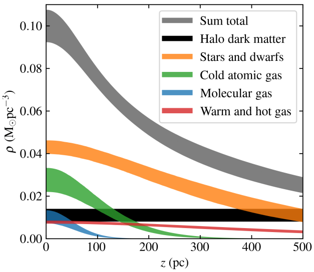

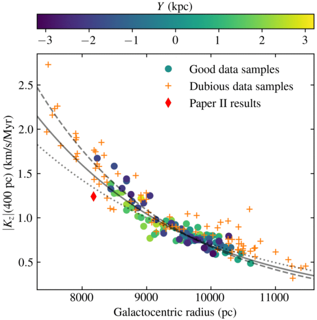

Constraining the Galactic potential by stellar streams

Since 2000, more than 100 tidal streams have been discovered in the Milky Way.

Since stars in a stream trace [nearly] the same orbit, they can be used to probe the Galactic potential [Ibata+ 2001; Koposov+ 2010; Law & Majewski 2010; Gibbons+ 2014; Bovy+ 2016; Malhan & Ibata 2019; etc.]

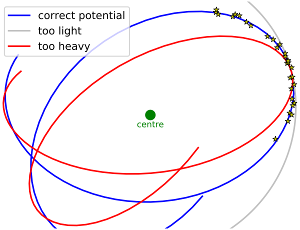

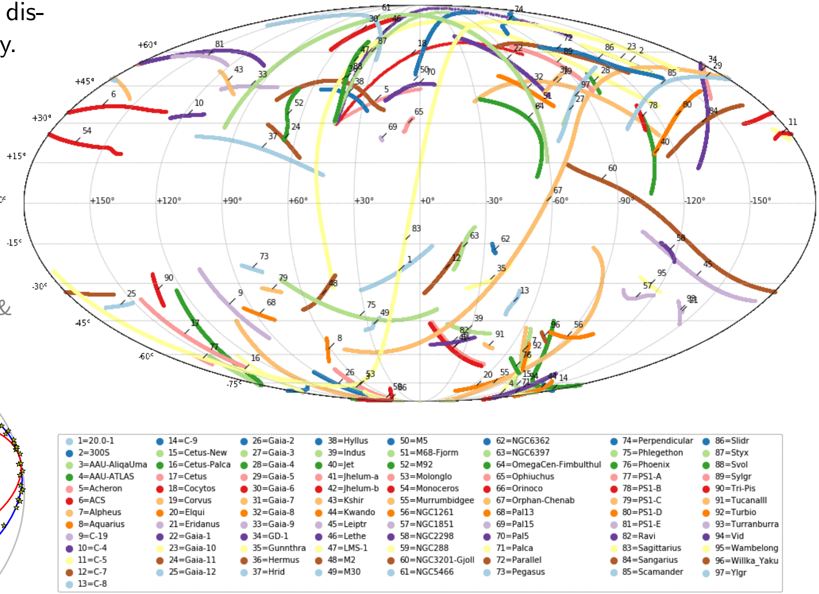

GalStreams library [Mateu 2022]

Constraining the Galactic potential by stellar streams

Caveat: streams in the outer Galaxy are affected by the recent LMC passage

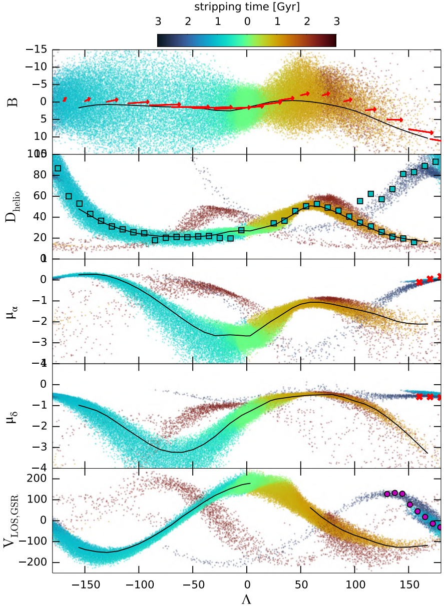

Sgr stream [Vasiliev+ 2021]

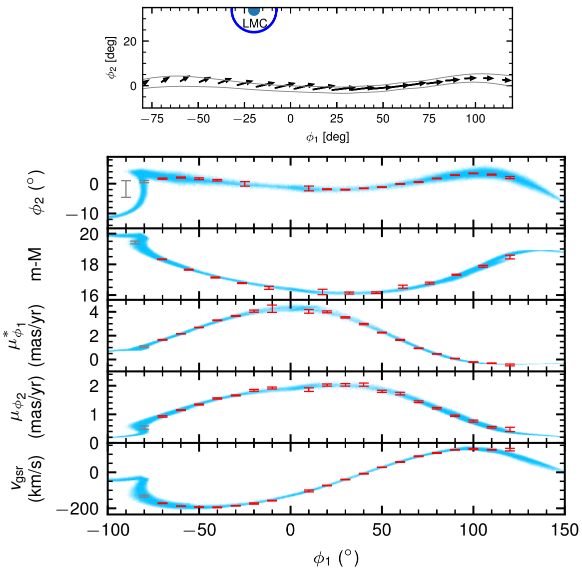

Orphan stream [Erkal+ 2019; Koposov+ 2022]

Constraining the Galactic potential by stellar streams

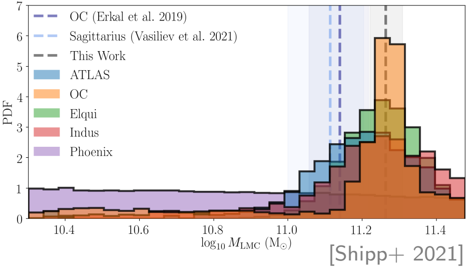

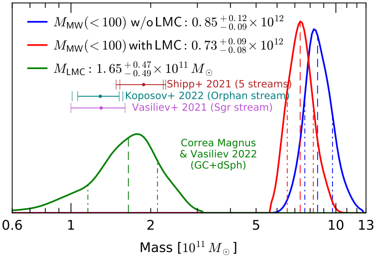

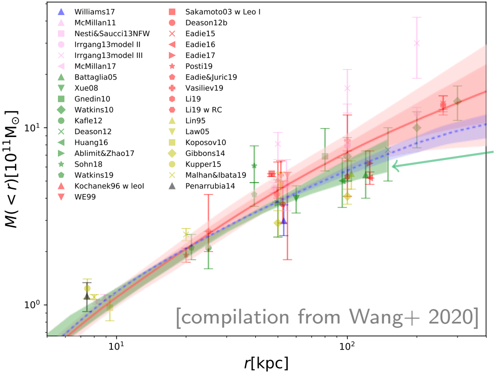

GC+dSph (+LMC rewinding) [Correa Magnus & Vasiliev 2022]

Sgr stream (incl. LMC) [Vasiliev+ 2021]

Orphan stream (incl. LMC) [Koposov+ 2022]

The LMC appears to have a mass of $(1\text{–}2) \times 10^{11}\, M_\odot$, while the Milky Way is $\sim 10^{12}\, M_\odot$ (lower than many earlier estimates). Neglecting the LMC perturbation biases the Milky Way mass up by $10 - 20\%$ [Erkal+ 2020].

Summary

enormous progress on the observational side

needs to be matched by improvements in modelling techniques!

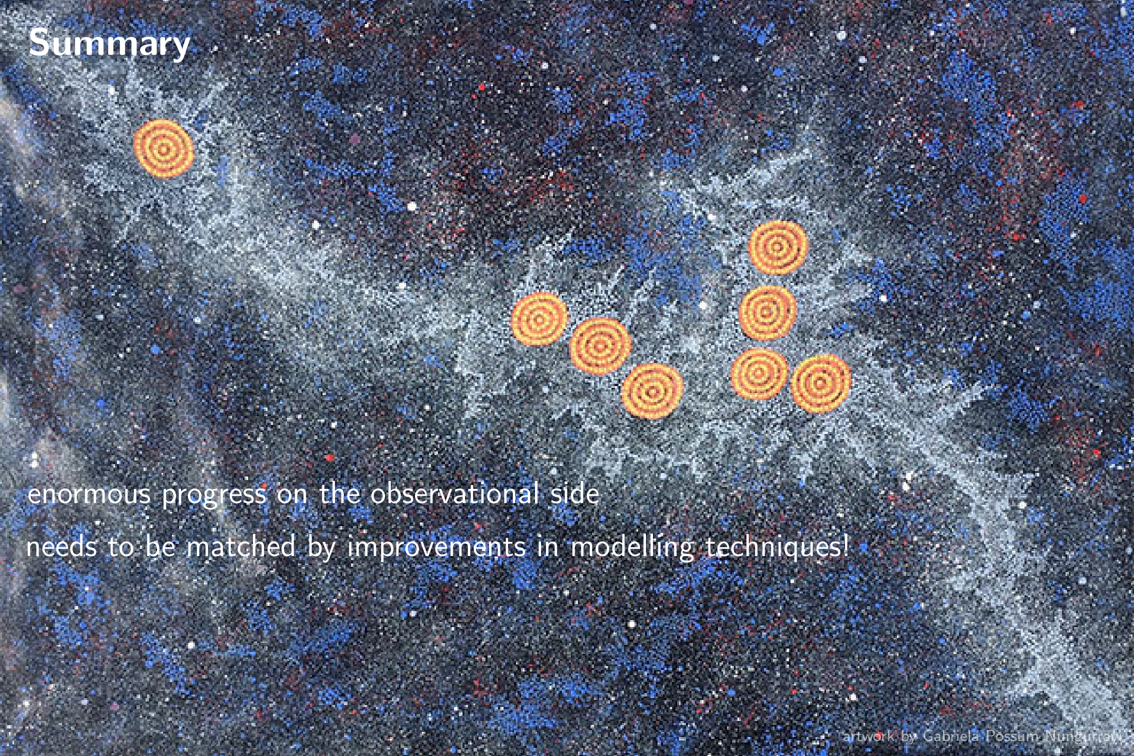

artwork by Gabriela Possum Nungurrayi